university of groningen

Bachelor's Thesis | April – July 2024

ADHESION OF ANISOTROPIC MICELLES IN STICKY MICROCHANNELS

Alexandra Danilov

S-Number: S4656156

E-Mail: a.danilov@student.rug.nl

University of Groningen, Micromechanics Unit of the Zernike Institute for Advanced Materials, Biomaterials and Biomedical Technology (BBT), Groningen, The Netherlands.

Thesis Supervisor: **Dr. Andrea Giuntoli**

Daily Supervisor: **Utku Gurel PhD**

Primary Examiner: **Dr. Andrea Giuntoli**

Secondary Examiner: **Prof. Dr. Ir. Erik van der Giessen**

I Abstract

Polymeric micelles, formed by the self assembly of block copolymers, play a crucial role in science, particularly in nanomedicine, as drug carriers due to their core-shell structure. There has been a lot of research done on the benefits and disadvantages of using spherical micelles in drug delivery, whereas non-spherical polymeric structures have received little to no attention in this field. Drug delivery in biological systems is a very complex process that includes multiple stages: loading of drug into the micelle and its injection in the bloodstream, diffusion to the target organs and cells and final drug release. In this study, we are exploring the first stage of micelle-mediated drug transportation, with a focus on the absorption of the polymers to the blood vessel membrane. Using a very simplified molecular dynamics system, this paper investigates the adhesive behavior of polymeric micelles with various aspect ratios (AR) in sticky microchannels simulating blood vessels. Our aim was to analyze how different micelle shapes, adhesion strengths, and channel sizes affect micelle behavior during the drug delivery process. We generated polymers of five different ARs (1, 2:1, 1.6:1, 1:3, 1:4.75) in channels of two different sizes, assessing their mean squared displacement (MSD) and the resulting slopes. The former will help us determine the distance a micelle travels before getting stuck, while the second will help identify the first attributed adhesion strength value (critical ASV) at which each micelle adheres to the wall. The results indicate that micelles with ARs of 1 and 1:4.75, attributed to the shortest and longest of the polymers, exhibit the highest critical ASV before adhering to the channel walls. This could suggest better permeability factors for those micelles, allowing them to travel longer distances in narrower vessels before getting stuck and absorbed into the target organ or cells. Conversely, micelles with ARs 1.6:1, 2:1, and 1:3 adhere more quickly and would be more suitable for use in drug transportation to highly permeable organs or tumors. Our findings highlight the influence of micelle shape on adhesion and provide insights for optimizing drug delivery systems. Future work should address the limitations of the current model, such as improving simulation parameters to obtain slopes of realistic non-zero values and explore more complex situations to better reflect physiological conditions, for example incorporating realistic blood flow dynamics and experimenting with additional channel sizes and micelle shapes .

I Table of Contents

II Table of Figures

1. Introduction

Polymeric micelles are an important class of macromolecular nanostructures formed by the self-assembly of amphiphilic block copolymers in an aqueous environment [1][2][3]. These block copolymers consist of both hydrophilic and hydrophobic units. Due to their self assembly behavior and their particularly core-shell structure, in which the hydrophobic part of the block copolymer forms the core of the micelle, whereas the hydrophilic portion forms the outer shell, polymeric micelles are important structures widely used in the world of science [4][5][6]. In nanomedicine, polymeric micelles act as drug carriers for drug transportation in vivo, exhibiting numerous advantages compared to conventional drug delivery systems (tablets, capsules, syrups, ointments, etc) such as selective targeting, reduced side effects of drugs, easy loading of hydrophobic medication, stability towards dilution and cheap and easy preparation [1][7][8].

Normally, polymer micelles come in spherical shapes, having been studied extensively for the past decades [9]. Their size plays a key role in their efficacy since, for example, micelles that range from 30 to 100 nm can accumulate with ease in high permeable tumors, whereas poorly permeable tumors can only be penetrated by micelles with dimension of 30 nm [10]. Because of the very shallow channels or pores they sometimes have to pass through to reach the desired destination in the body, one downside of using spherical micelles in drug delivery is their limited drug loading capacity [11]. Pioneering studies show that nonspherical nanocarriers show great promise as cancer drug delivery vectors [12]. In a study done in 2011 by Chauhan et al., nanospheres (35 nm) and nanorods (15 × 54 nm) with the same coating and charge were used for targeting tumors. It was found that nanorods penetrated tumors faster than nanospheres due to improved transport and reduced viscous drag near the pore vessel walls, which are the walls of the blood vessels within the tumor that have tiny pores or gaps. [13].

The optimization of micelles in drug delivery systems remains an ongoing challenge for scientists and continues to evolve [14]. Using nanoparticles (NPs) for drug delivery requires improved NP properties, such as material, size, shape, and surface modification. These factors need to be tailored to achieve the desired functions, such as the ability to circulate in the blood, target specific tissues, enter target cells, and release drugs under certain conditions [15][16].

Before getting absorbed to the target organ or tumor, micelles pass through capillaries, where they adhere to their walls. The diameter of a capillary typically ranges from 5 to 12 μm. However, tumor capillaries are typically larger and more irregular than those in normal tissues, ranging from 10 to 50 μm in diameter, some even reaching 200 μm [17][18]. Typical time spent by drug-delivery carriers in the bloodstream varies extensively on micelles' morphology and surface modifications [19]. Most importantly, small differences in size and charge, two of the most basic parameters of NPs, can significantly influence biological effects on cellular uptake and biodistribution [20]. A study done by He et al revealed that nanoparticles with greater surface charges and larger sizes had a higher likelihood of being engulfed by macrophages. Conversely, nanoparticles with a diameter of around 150 nm and a mild negative charge were more prone to accumulate effectively in tumors [21]. The size limitations of these spherical nanoparticles imply a limit to the drug loading capacity of a micelle. Hence, studies have been done to assess the role of nonspherical NPs in drug delivery systems.

To investigate how carrier geometry affects endothelial targeting, Shuvaev et al. tested nanoparticles (NPs) of various shapes, including disc-shaped and flexible polymeric filomicelles made from polyethylene oxide diblock copolymers [22]. Their results showed that elongated carriers (mainly large disc-shaped and filamentous cells with a length from 3 to 7.5 μm) exhibit longer residence times in the bloodstream than spherical carriers (~150 nm). Because of the decreased interaction with phagocytes and the blood vessel wall compared to the spherical structures, the elongated carriers experience a slower clearance from the circulation, providing a longer circulation time in the bloodstream. Prolonged circulation time offers more chances for micelles to reach the target tissue, extends the drug release period [23], prolongs their effectiveness as imaging contrast agents [24], or enables extended interaction with the blood [25].

Even though the shape of nanoparticles has been identified as a key factor influencing pharmacokinetics [26][27], the behavior of anisotropic polymeric micelles used as drug carriers in biological systems has not been researched extensively yet [28]. Hence, there still needs to be a clear answer to the advantages rod-shaped polymeric nanocarriers can bring to future drug

delivery systems, particularly regarding transportation in microchannels and tissue penetration in cancer therapy. Drug delivery is a very complex process that includes multiple stages i.e. injection of drug (and micelles) into the bloodstream, diffusion to the target organs and cells and finally, drug release to the desired part of the body [28]. In this paper we are going to focus on the first stage aforementioned, namely the absorption stage of a micelle to the blood vessel wall. Using very simplified molecular dynamics (MD), we are going to analyze the adhesive behavior of 5 different aspect ratios (AR) of polymers (1, 2:1, 1.6:1, 1:3, 1:4.75) in sticky microchannels of two different sizes, mimicking a blood vessel or a capillary. We will quantify the probability of adhesive events, as polymer adsorption to the channel wall, as a function of simple parameters such as micelle shape, adhesion strength and channel size.

In this study, we focus on the relationship between the shape of the micelles and its effect on circulation time at given adsorption strength, confinement ratio, and bloodstream strength. Sakamoto et al used similar conditions to explore macrophage uptake by controlling aspect ratio of graft copolymer micelles [29]. Their findings emphasize that cylindrical micelles with an aspect ratio of 2.4 are the least susceptible to macrophage uptake compared with both their longer counterparts (AR 5.6, AR 10.8) and spherical micelles (AR 1). Another study, by Goroya et al, develops and validates a mathematical model to understand how blood flow affects nanoparticle adhesion and retention [30]. Their results suggest that larger nanoparticles are more effective in sticking to their targets in the bloodstream, which can help in designing better drug delivery systems and reducing reliance on animal testing. Compared to these two papers, that address macrophage uptake and the effects of blood flow on NP adhesion and retention, our focus is on examining how the shape of micelles affects adhesion times, specifically comparing the behavior of isotropic and anisotropic micelles under identical conditions, during the first stage of drug delivery.

The principal methods applied imply the use of the mean squared displacement (MSD) and its slope values to determine the distance traveled by the micelles before getting completely stuck and, respectively, the attributed adhesion strength values (critical ASVs) at which the polymers adhere to the walls of the channel first. The main findings of this study indicate that micelles

with ARs of 1 and 1:4.75, corresponding to the shortest and longest polymers, exhibit the highest critical ASVs. This suggests better permeability factors for these micelles, enabling them to travel longer distances in narrower vessels before getting stuck and absorbed into the target organ or cells. Alternatively, micelles with ARs of 1.6:1, 2:1, and 1:3 present lower critical ASVs, adhering more quickly to the channel walls, making them more suitable for drug transportation to highly permeable organs or tumors.

2. Simulation model & Methods

2.1 Molecular dynamics framework

Molecular dynamics (MD) is an important and widely used computer simulation tool used to study the physical movements of atoms and molecules [31]. This theoretical method allows scientists in the fields of chemistry, physics and biology to model the detailed microscopic dynamical behavior of many different types of systems, including gases, liquids, solids, surfaces, and clusters. MD methodology is based upon classical mechanics, particularly Newton's law of motion; every atom in this system is represented by a point-mass, which visually resembles a bead, and its trajectory is described by solving Newton's equations of motion. These equations completely determine the full set of positions and velocities of the atoms as functions of time (t) and thus specify the classical state of the system at a given t. In the context of molecular dynamics, we use coarse-grained simulations, a technique used to simplify and speed up the computational study of complex molecular systems by reducing the level of detail in the model. These simulations progress in small time steps, usually in the order of femtoseconds (a quadrillionth of a second), where at each step, the positions and velocities of the atoms are updated based on the calculated forces [32]. The forces acting on atoms are derived from potential energy functions which describe the interactions between particles. Common potentials include the Lennard-Jones potential, Coulombic interactions, and bonded interactions like bonds, angles, and dihedrals. To visualize our micelles and our simulations, we used a data visualization and analysis software for molecular dynamics called OVITO [33]. OVITO is a 3d graphics desktop application used by scientists in various different disciplines such as computational

materials science, engineering, physics and chemistry to view, edit and analyze their particle-based simulation models.

2.2 Simulation model

2.2.1 Micelles

The 5 different aspect ratios chosen for the polymeric micelles can be seen below in Figure 1. Their calculation has the form of "y:z", simplified until either y or z reaches 1. The y value represents the polymer's width, whereas the z value depicts its length. Figure 2 showcases how the ARs of the micelles are calculated, using polymer 4 as an example. For the polymer with the aspect ratio of 1, we generated a star polymer, while for the other four, we used the structure of bottlebrush polymers. Each polymer consists of 240 beads, each representing one atom in the coarse-grained simulations, divided into two types. The first one, type 1, shown as the red beads in Figure 1, makes up the core beads, while the second one, type 2, represented by the blue beads in Figure 1, forms the shell of the micelles. The two types are marked as different for an easier attribution of the specific bonds needed to create the correct structures of a star polymer and of a bottlebrush polymer. The star polymer has one atom bead as the core, whereas the bottlebrush structures have different backbone chain lengths (L). Micelle 1, the star polymer, features a shell composed of 16 arms, each made out of 15 beads, while the other 4 micelles, the bottlebrushes, have shells made out of varying numbers of side chains. For polymers 2 to 5, the selected backbone (L) and side chain (M) lengths, measured in number of beads, are as follows: 5 and 47, 10 and 23, 24 and 9, and 40 and 5, respectively.

All parameters used in our simulations can be measured in Lennard-Jones units (LJ). LJ units are a system of non-dimensional units commonly used in molecular dynamics simulations to create a simplified and standardized way of describing molecule interactions. This molecular dynamics system uses three main quantities namely energy (ε), distance (σ) and mass (m) that are scaled based on the Lennard-Jones potential, defined as follows: $U_{LJ}(r) = 4\varepsilon[(\sigma/r)^{12} - (\sigma/r)^{6}]$. This potential represents a mathematical model that describes the interaction between a pair of neutral atoms or molecules. In this simulation, all parameters are set in lj units, being

standardized relative to the intrinsic properties of the system. The bond interaction between two linked beads are described using finitely extensible nonlinear elastic (FENE) potentials, $U_{FENE}(r) = -0.5kR_0^2 \ln[1-(r/R_0)^2]$, where r denotes the bead-bead distance, k represents the spring constant and R_0 is the maximum bond length for r. In this case, k is chosen to be 30.0 units in the LJ system and the maximum separation R_0 is 1.5 units in the LJ system.

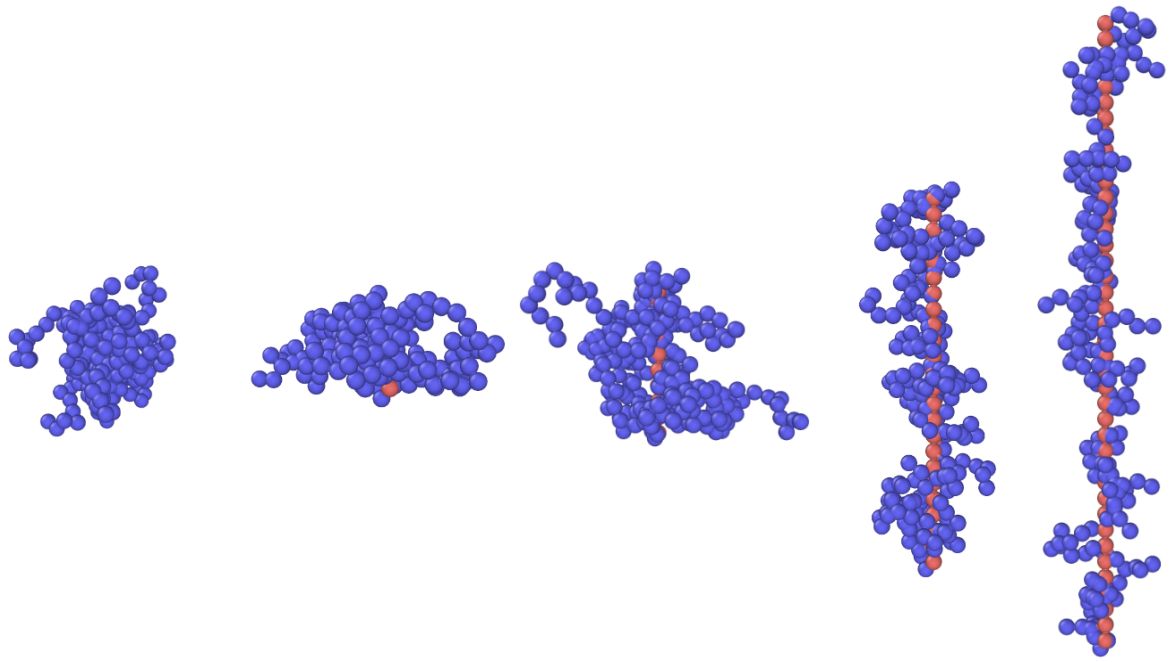

Figure 1- chosen aspect ratios for the polymeric micelles; vertical axis represents the length of the micelle, while the horizontal axis depicts the width; from left to right: micelle 1- sphere star polymer of aspect ratio (AR) of 1, micelle 2 - bottle brush polymer L5M47, AR 2:1, micelle 3 - bottlebrush polymer L10M23, AR 1.6:1, micelle 4 - bottlebrush polymer L24M9, AR 1:3, micelle 5 - bottlebrush polymer L40M5, AR 1:4.75

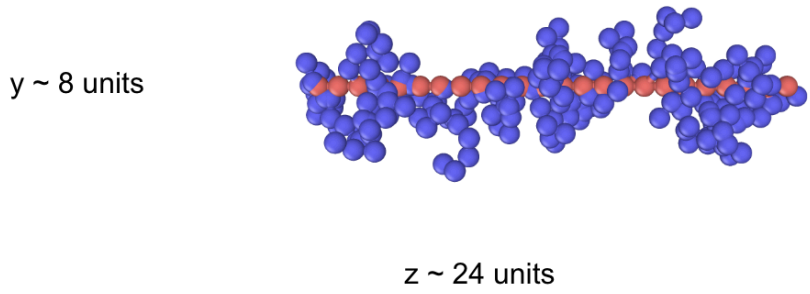

Figure 2 - measurements of micelle 4 in its relaxed position (z = 24) and (y = 8), having an AR of 8:24, simplified to AR = 1:3

2.2.2 Simulation channel

Besides the previously described polymers, the simulation setup also consists of a microchannel (Figure 3) that has walls made out of a third different type of atoms (type 3) to simulate friction between a micelle and (pore) vessel walls. As before, the different types of atoms are made to distinguish different particles and their roles from one another (core beads, side chains and walls). The role of the friction is to simulate the resistance encountered by a micelle moving through blood while interacting with the walls of a blood vessel.

The microchannel and the simulation are generated using a Large-scale Atomic/Molecular Massively Parallel Simulator, also known as LAMMPS. LAMMPS is a classical molecular dynamics code with a focus on materials modeling that can be used to model atoms or, more generically, as a parallel particle simulator at the atomic, meso, or continuum scale [16]. Two different channel sizes are tested with dimensions (Lx, Ly, Lz) and (Dx, Dy, Dz), where, for channel 1, Lx = Ly = 20, Lz= 200 and for channel 2, Dx = Dy = 30, Dz= 200. The elongated polymers are initially placed parallel to the direction in which the wall is being formed. For the atoms of the polymers to not interfere with the atoms of the walls while they're being created, an initial relaxation of the former would suffice. This relaxation is performed with the command "pair_style soft 0.1". The soft potential is used to allow soft interactions between atoms. The parameter of 0.1 indicates the force constant for the soft potential, which, being set so low, allows particles to overlap more easily without generating large repulsive forces. The atoms that

make up the walls are then created with the “create_atoms” command, but not before defining a face-centered cubic (FCC) lattice that defines the spatial arrangement of the particles in the simulation channel. The command used for the lattice is “lattice fcc ${rhostar}”, where “ ${rhostar}” represents the reduced density for a FCC lattice, which is derived from the diameter of the particles. Moreover, the atoms that make the channel should not move or react to any force applied to them, hence, the beads are tethered via a stiff harmonic spring to the lattice sites. The utilized command is “fix tether subs spring/self 1000.0” where 1000.0 indicates a relatively high force constant that will have atoms pulled back to their initial positions with a strong force if they move away. This will make sure the atoms remain rigid, tightly bound and fixed in place. The interactions between the non-bonded atoms are described through the “pair_coeff” command. Based on the Lennard-Jones potential, for the interactions between the three different types of atoms, the sigma (σ) parameter, representing the distance at which the potential is 0, is set to 1.0, and the cutoff value is set to 2.5. The epsilon (ε_{wall}) parameter is defined as the depth of the potential well, representing how strong the attractive forces between two non-bonded particles are. In our simulation, ε_{wall} is the main value that describes the stickiness of the microchannel. Because in this paper we want to assess and compare the behaviors of the micelles at the absorption stage in different situations, one of the parameters we are changing is ε_{wall}, which will take values from 1 to 10. The force flow is generated with the “fix addforce 0.0 0.0 1.0” command in LAMMPS. This command is used to give a constant push to the polymer’s atoms throughout the whole simulation, mimicking Poiseuille flow. Poiseuille flow describes the laminar flow of a viscous fluid through a cylindrical pipe. Capillaries, with their small diameters and relatively slow flow rates, often exhibit conditions suitable for Poiseuille flow, confirming the beneficence of the use of the aforementioned command [35]. The direction of this flow is set by the non-zero parameter, in this case, 1.0. The first 0.0 denotes that the flow in the x direction is 0, whereas the second 0.0 implies no flow in the y direction. Because our simulation channels are built parallel to the z axis, the direction of the flow is also set in the z axis. Our simulations are run for extended durations, and thus the length of the simulation channel is insufficient to encompass the entire travel distance. For this reason, a periodic boundary is attributed to the specific direction using the command “boundary f f p”, where “f” means fixed and “p” denotes periodic. Therefore, the simulation can run infinitely in the same channel. In real life, the velocity of blood measures at about 0.003 - 0.01 cm/s in capillaries, but for simplicity reasons

regarding later measurements, a value of 1 was attributed to the force. Because velocity is not a parameter we are manipulating in this paper, a standard, relatively slow force was chosen to give a constant push to the particles. Consequently, the different micelles' behavior in the system can be differentiated more easily.

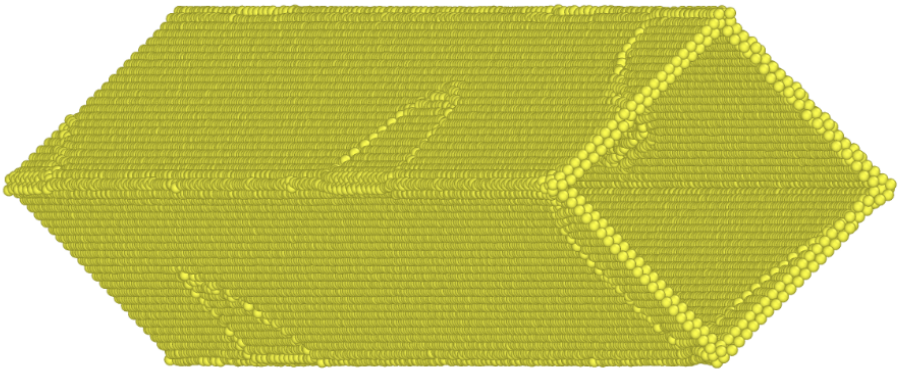

Figure 3 - simulation channel made out of type 3 polymers

2.3 Simulation setup

For every AR of our micelle we ran the simulation for 10 ε_{wall} values (1 to 10), for both channel sizes. To evaluate the consistency of the micelles' behavior within one channel, the simulations were replicated for 100k, 200k and 300k simulation steps to determine if the adhesive trends of the polymers remained the same. This gave us a total of 300 simulations. For time management and results efficiency reasons, we used signac, an open-source library designed to manage and organize large-scale data and workflow management tasks in scientific research, to streamline our data workflow, ensuring efficient organization and analysis of our computational experiments [36]. For each micelle, ten different jobs were generated (ε_{wall}=1, ε_{wall}=2, …, ε_{wall}=10) each containing the same simulation with different values for how strong ε_{wall} is. After the completion of this step, the simulations are run and post processed. This whole procedure is repeated for all ARs, at three simulation runtimes, for both channel sizes.

2.4 Post-processing and methods

The post processing begins with the calculation of the mean squared displacement (MSD) for each job which assesses the average squared distance that the polymer travels at different time points from its original position. The formula used is $\mathrm{MSD}(t) = \frac{1}{N}\Sigma_{i=1}^{N}(|r_i(t) - r_i(0)|^2)$, where N is the number of atoms the micelle has, $r_i(t)$ is the position of the atom i at time *t* and $r_i(0)$ is the initial position of the same atom. The higher the MSD value of the micelle gets, the longer the distance traveled from the initial position. For a better understanding of the behavior of the polymer, a graph of all 10 individual mean squared displacements for all ε_{wall} as a function of time is generated. By just looking at it, with no further analysis, we can tell which particles get completely stuck to the walls of the microchannel. As illustrated in Figure 4, a constant mean squared displacement (MSD) value over time indicates that the particle has adhered to the walls. Moreover, further examination is needed to determine the range of ε_{wall} values within which the critical ASV ($\varepsilon_{wall}^{critical}$), at which the particle adheres first, is found.

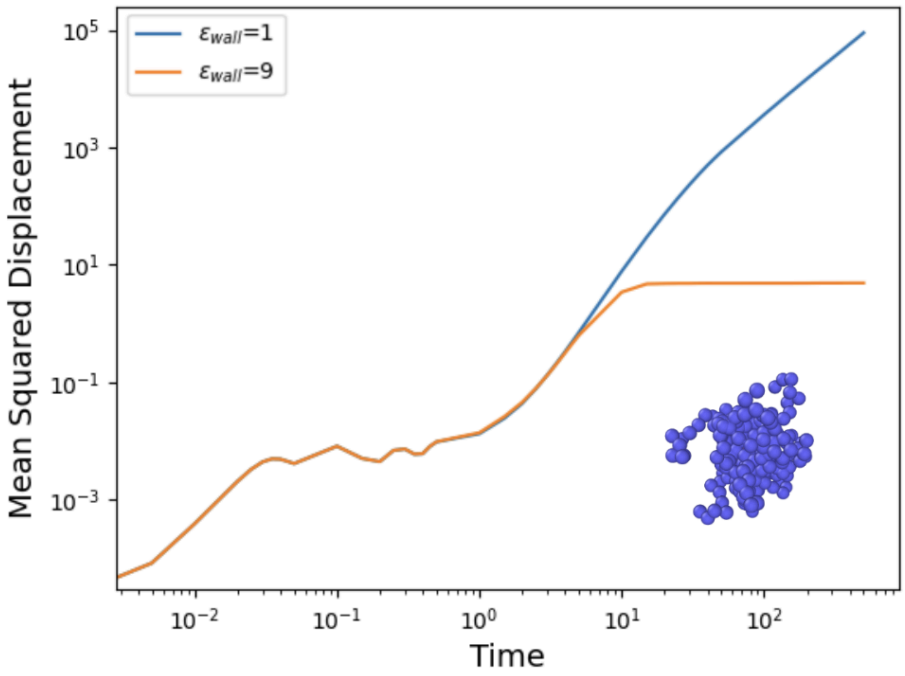

Figure 4 - Mean squared displacement calculation calculation as a function of time for micelle 1 depending on ε_{wall}; for ε_{wall}=1, micelle does not adhere to the channel wall, whereas for ε_{wall}=9, the constant MSD indicates the polymer gets stuck; simulation performed for 100k steps

The next step in the post processing would be comparing the MSD values obtained from all ARs (for the same simulation runtime and channel size). This can be achieved by generating a plot of the final MSD values for all simulations as a function of ε_{wall} for each micelle. The obtained graph will help compare the total traveled distance of the micelles under the same conditions. To evaluate the consistency of their behavior within one simulation channel, the graph was replicated for 200k and 300k simulation steps to determine if the trends with varying ARs and ε_{wall} remained the same. This was performed for both simulation channels. An interpolation of the MSD points of each ε_{wall} is done in order to more accurately calculate the corresponding slopes (between consecutive points on the MSD graph) later. Using the UnivariateSpline function in python and computing the logarithmic values of the msd and time points we obtained smooth individual splines for all simulations run. Figure A1 in the appendix shows the difference in plotting between the mean squared displacement points and the interpolated MSD points. Using the data plotted in panel b) on the smooth spline line for slope calculation between consecutive points ensures reliable determination of the regimes of particle motion micelles find themselves in during simulation time.

The last step in our post processing, also described above, is calculating the slopes between all consecutive points on the interpolated graph. This will help us recognize what regime of particle motion the polymers are in throughout the simulation. If the slope is smaller than 1, the particle is in the subdiffusive regime, while a slope greater than 1 indicates the particle is in the superdiffusive regime. A slope of 0 implies that the consecutive MSD values used in the calculation were identical, implying that the polymer does not move. More importantly, similar to how we compared the final MSD values, we will compare the last values of the obtained slopes to determine and evaluate at which values of ε_{wall} the micelles adhere to the channel walls. This approach will enable us to identify the range of ε_{wall} values within which $\varepsilon_{wall}^{critical}$ lies, allowing us to draw conclusions about the overall adhesive behavior of the micelles. The formula used for the calculation of the slopes is slope = $\Delta y/\Delta x$, where x belongs to the interpolated set of

the msd values, and y is part of the corresponding time set. Additionally, we can compare the results obtained from both channel dimensions to gain further insights.

3. Discussion & results

Figure 5 illustrates the average squared distance the 5 polymers travel as a function of ε_{wall}. As explained above in section 2.4, this figure helps determine which particles get completely adhered to the walls. Figure 6 and Figure 7 show the last mean squared displacement (MSD) values for each polymer aspect ratio plotted against ε_{wall} for simulations done in channel 1 and channel 2, respectively. For both figures, graphs (a) to (c) represent time steps from 100k to 300k. In both cases, the behavior of all micelles remains constant over time, supporting the validity of our data.

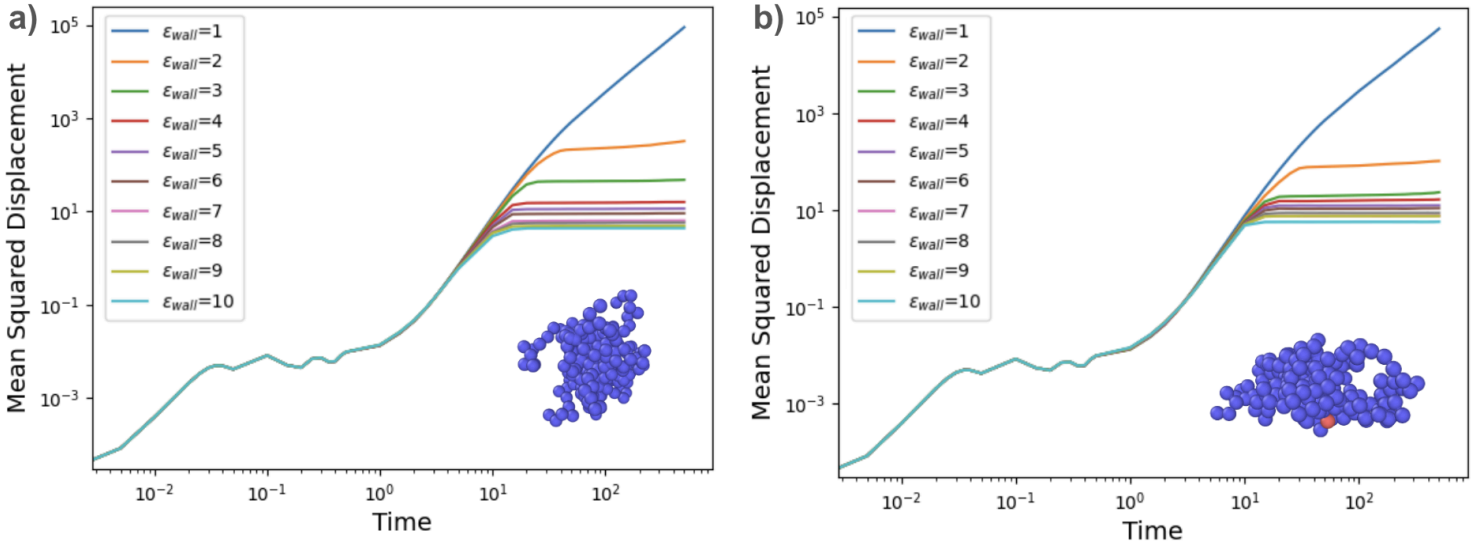

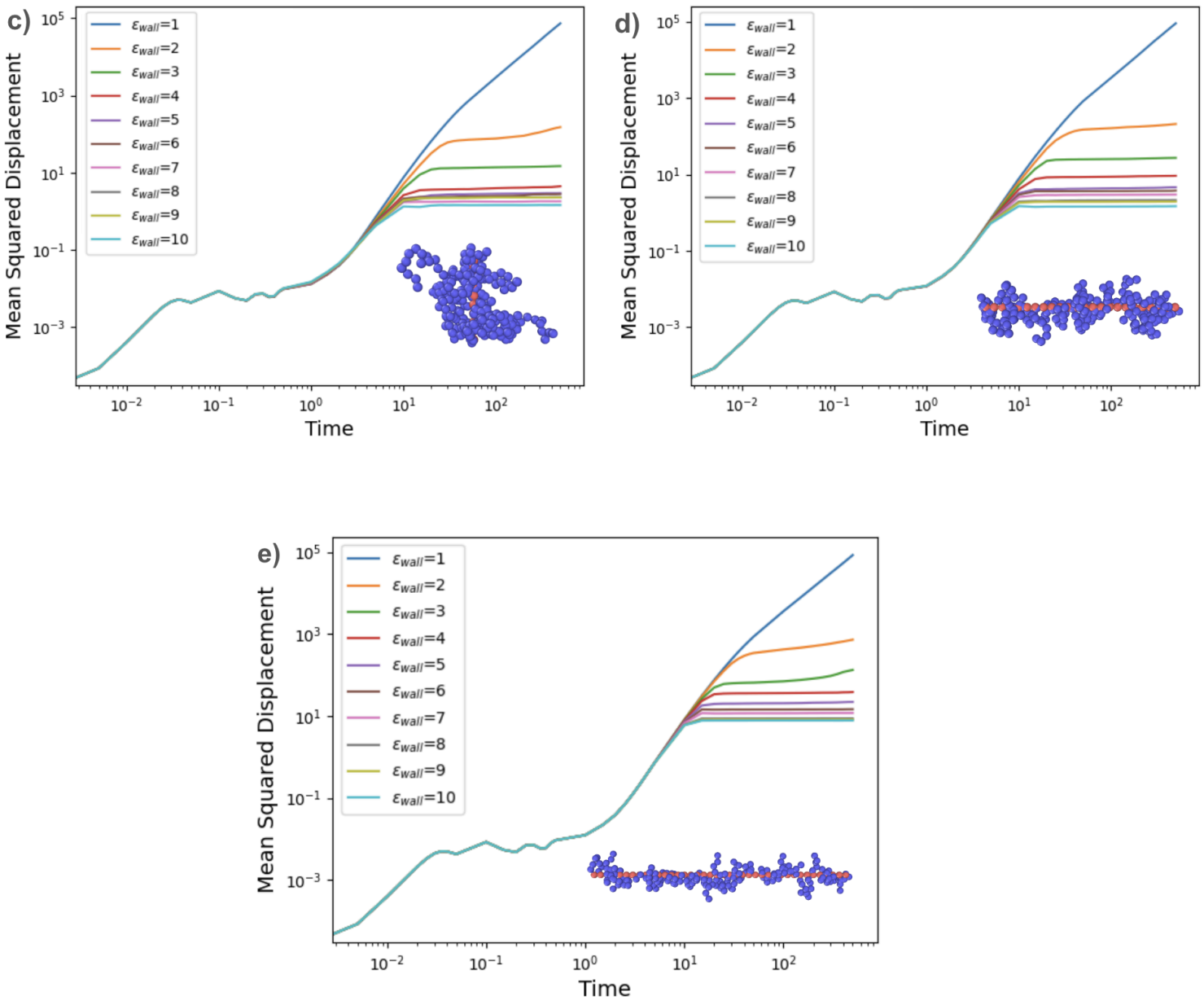

Figure 5 - Mean squared displacements for ε_{wall} from 1 to 10 plotted against time for a) polymer AR 1, b) polymer AR 2:1, c) polymer 1.6:1, d) polymer 1:3, e) polymer 1:4.75; 100k steps, simulation channel 1

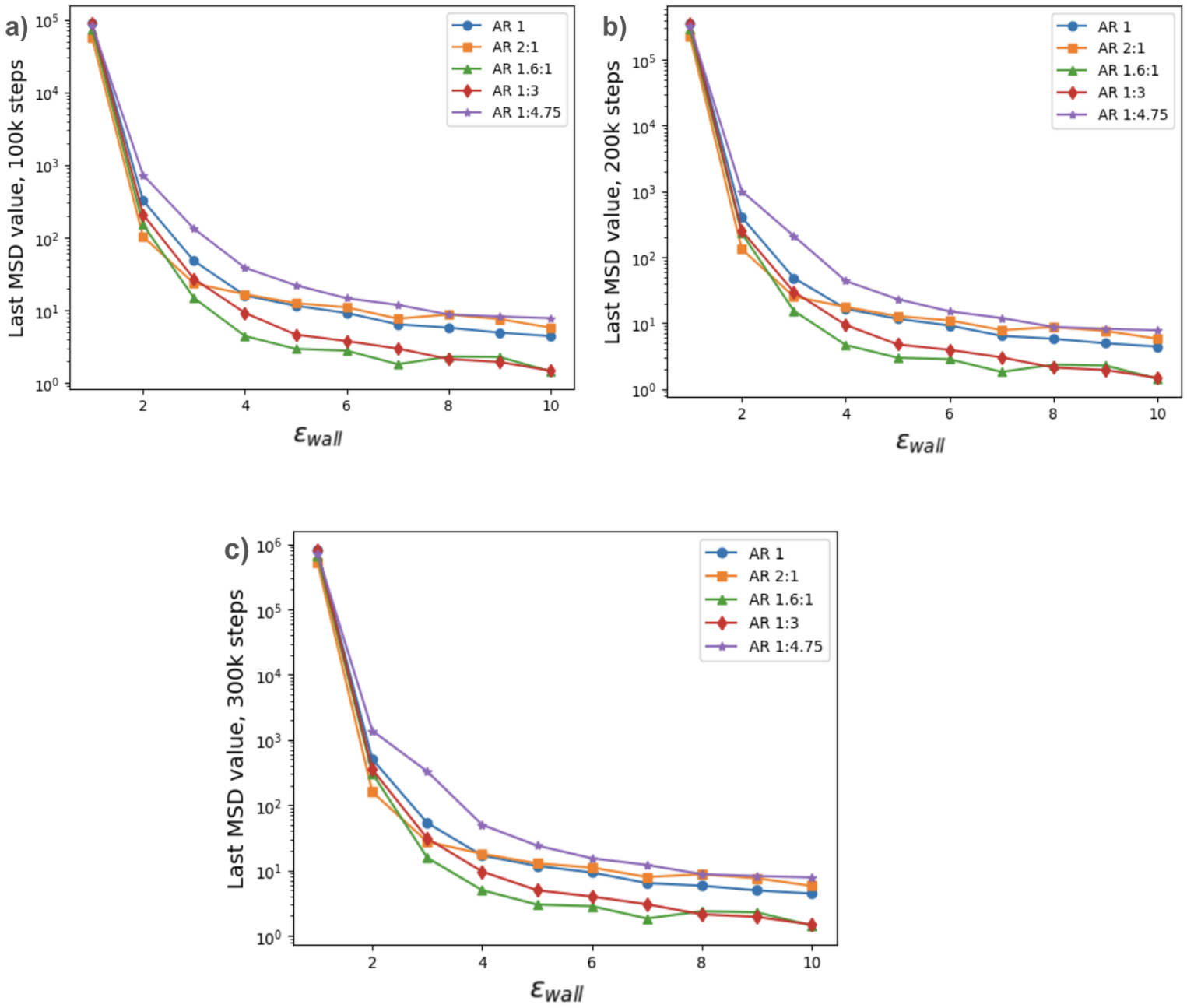

Figure 6 - Last mean squared displacement (MSD) values depending on ε_{wall} for all 5 polymers simulated in simulation channel 1 obtained after a) 100k steps, b) 200k steps and c) 300k steps

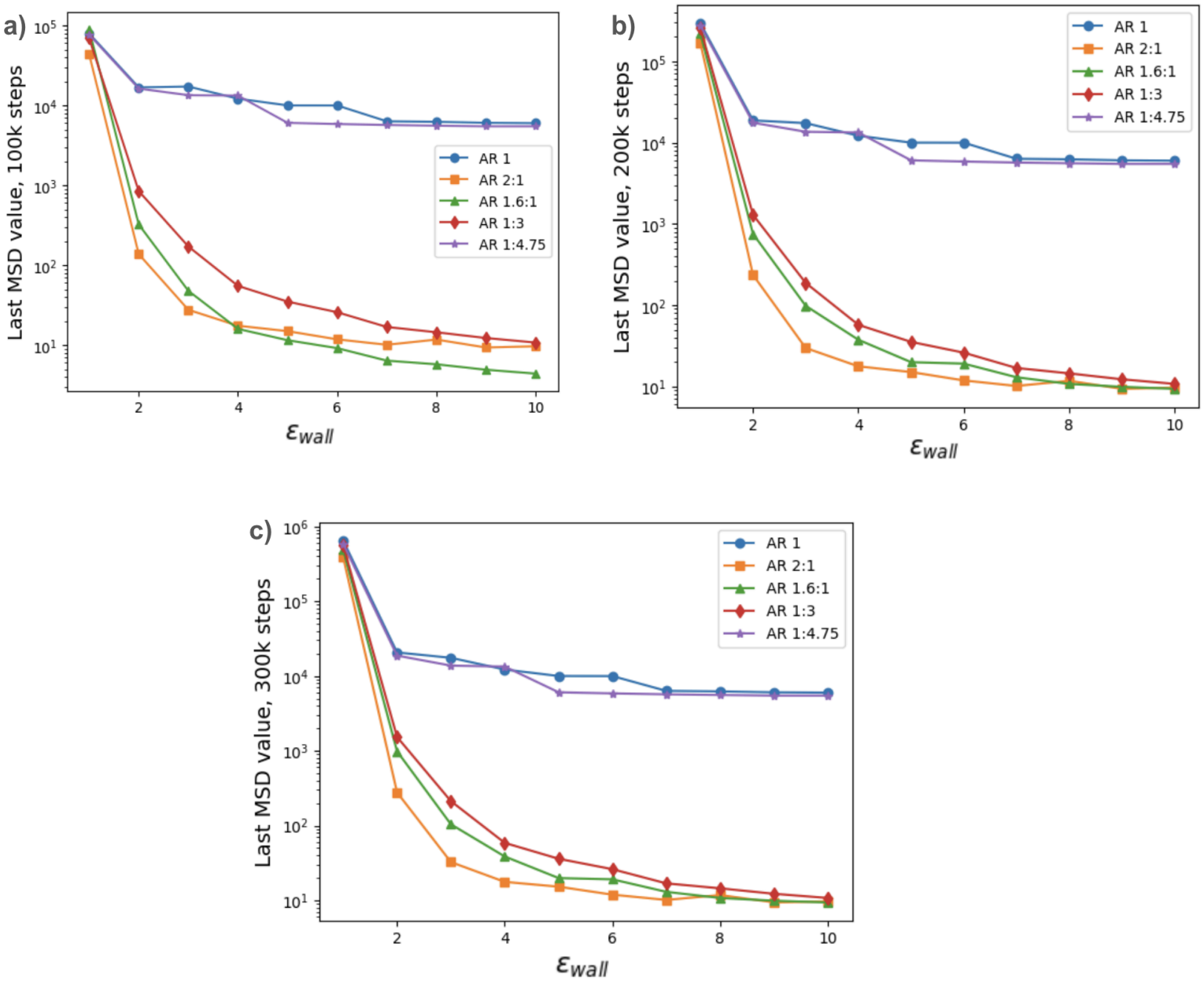

Figure 7 - Last mean squared displacement (MSD) values depending on ε_{wall} for all 5 polymers simulated in channel 2 obtained after a) 100k steps, b) 200k steps and c) 300k steps

Focusing on simulation channel 1, polymers with an AR of 1.6:1 and 1:3 tend to adhere to the channel walls the quickest, indicating they travel the least. Conversely, polymers with an AR of 1, 2:1, and 1:4.75, representing the two shortest and the one longest of the five micelles, take longer to stick to the walls. This delayed adhesion suggests a longer travel time for these

polymers, making them more suitable as drug carriers for targeted therapies due to a high retention efficiency. Tumors often have leaky vasculature, and due to the enhanced permeability and retention (EPR) effect that allows for better accumulation of micelles in tumors, drug carriers that stay in the bloodstream longer have a higher chance of penetrating these areas. Examining simulation channel 2, we observe similar polymer behavior, with polymer with AR 2:1 now exhibiting adhesion patterns akin to polymers with ARs 1.6:1 and 1:3. A notable difference is seen in the 1 polymer and the 1:4.75 polymer; although their behaviors remain comparable to each other, they adhere much later than the other three polymers. This late interaction with the walls of the channel confirms the fact that those two micelles could be described as having a better retention efficiency. One common characteristic among all of the graphs is that none of the micelles adhere to the wall when $\varepsilon_{wall} = 1$. Further in this discussion, we will analyze the ε_{wall} values at which micelles first adhere, thereby drawing more insightful conclusions about their adhesive behavior.

Figure 8 and Figure 9 show the final slope values for each polymer aspect ratio plotted against ε_{wall} for simulation channel 1 and simulation channel 2, respectively. In both cases, graphs (a), (b) and (c) indicate the runtimes 100k, 200k and 300k, measured in time steps. The 100k step simulations exhibit inconsistent behavior compared to the other two runtimes, which yield fairly similar data. This inconsistent behavior underscores the importance of conducting studies over longer periods of time. Due to the very high slopes obtained in all plots for ε_{wall} of 1, Figure 9 and Figure 10 provide a deeper examination for wall 1 and 2 respectively. They present the same plots for the same time steps, starting from $\varepsilon_{wall} = 2$ and $\varepsilon wall = 3$. This will help us determine precisely where, and if, our polymers adhere to the walls.

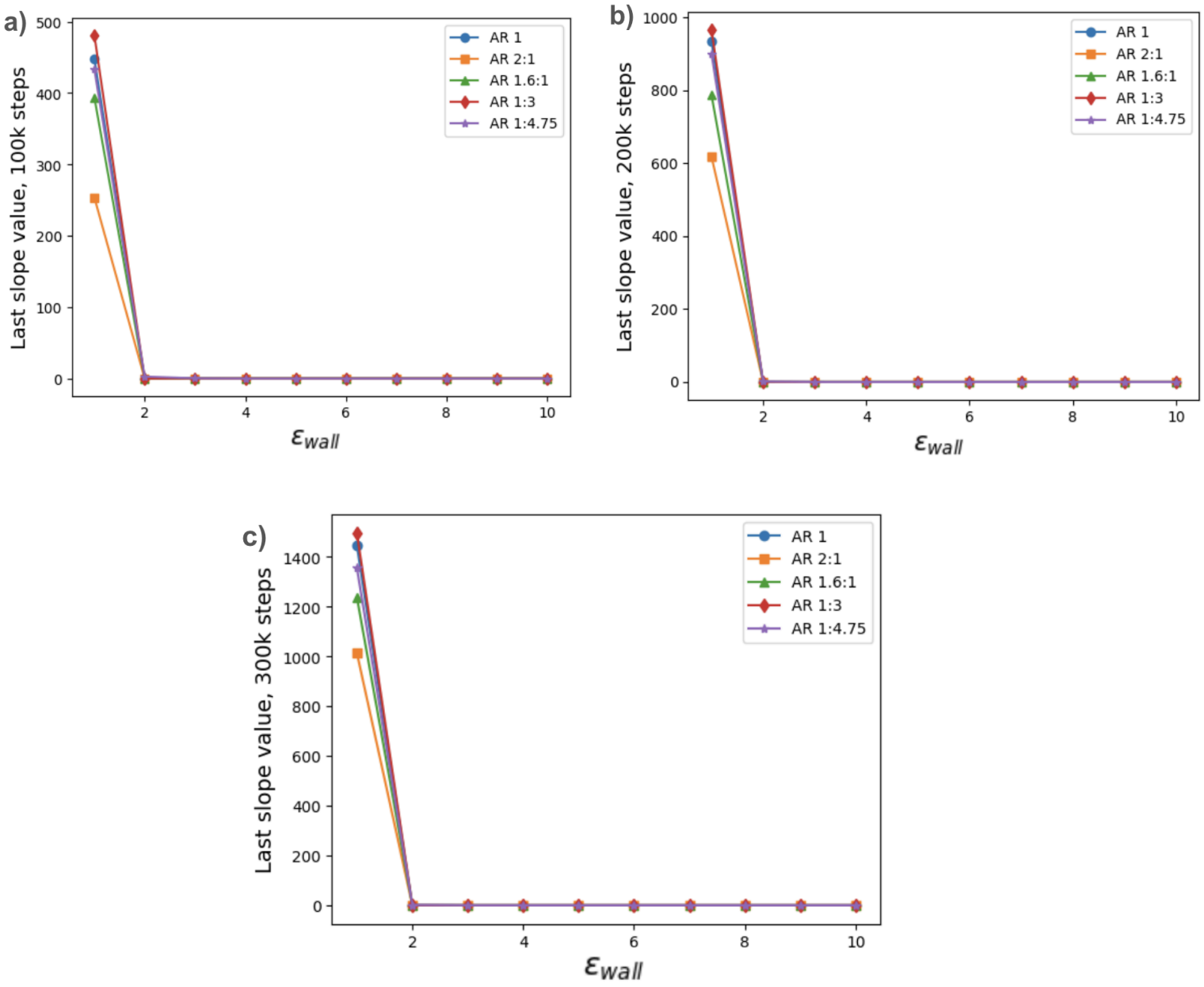

Figure 8 - Last slope values as a function of ε_{wall} for all 5 polymers simulated in simulation channel 1 obtained after a) 100k steps, b) 200k steps and c) 300k steps

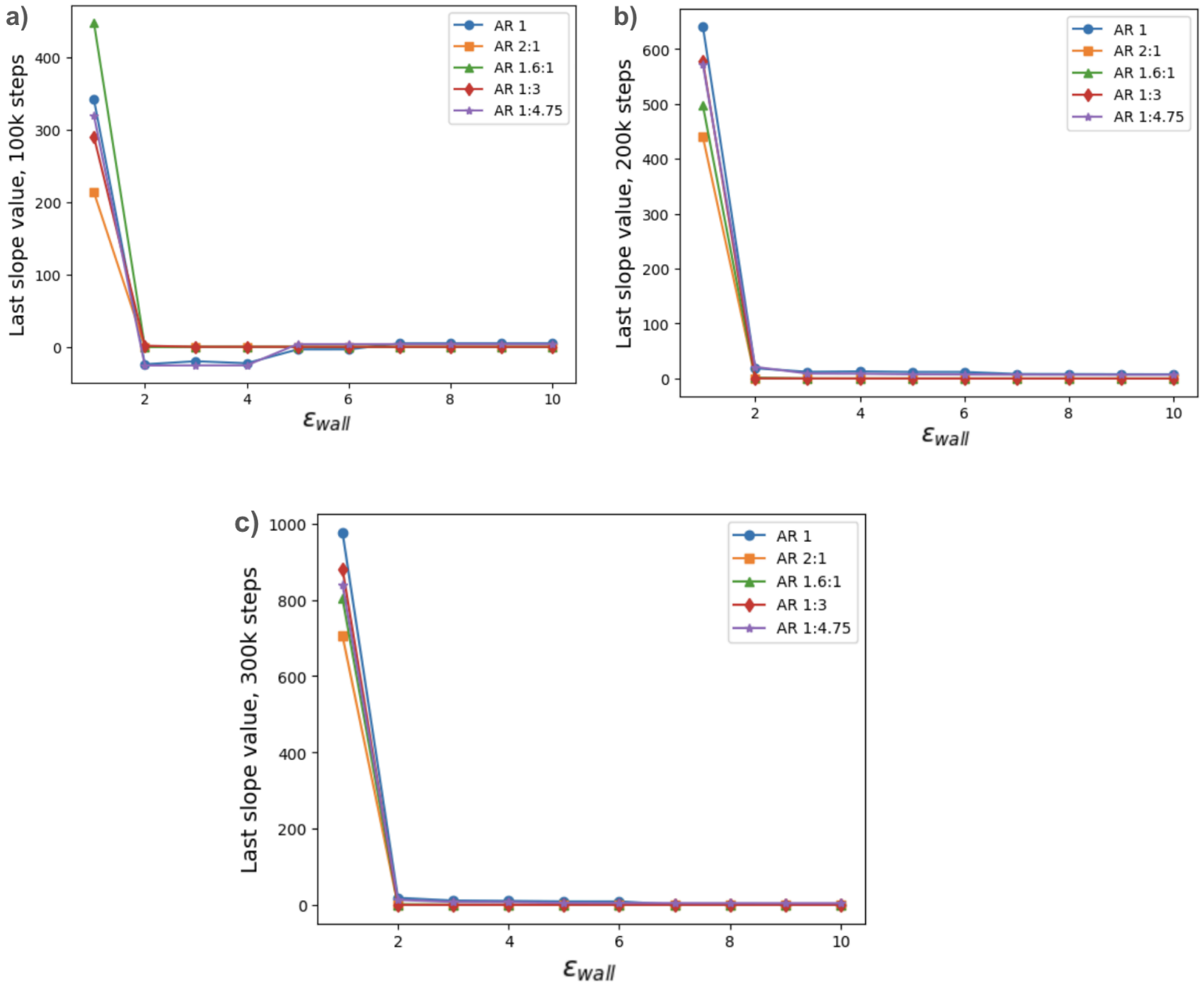

Figure 9 - Last slope values depending on ε_{wall} for all 5 polymers simulated in simulation channel 2 obtained after a) 100k steps, b) 200k steps and c) 300k steps

The very high slope values obtained for the ε_{wall} = 1 would theoretically denote a faster-than-ballistic velocity which is not present in our simulation setup. The limitation present here is in the calculation of the slopes from the interpolated values of the MSD. Due to the very

high mean squared displacement values achieved in simulations with ε_{wall} = 1 (on the order of > 10^4), the difference between consecutive interpolated points increases significantly. Consequently, even though the time intervals between successive points remain constant, the growing difference between these points results in increasingly inaccurate slope values. More in depth calculations are needed in order to get reliable non-zero values. Moreover, the high negative values observed in panel a) of figure 9 also do not make sense physically.

By first analyzing the micelles in channel 1 and examining Figure 8, we observe that the behavior of the polymers remains relatively constant over time. A more in depth look at the polymers, as shown in Figure 10, reveals that for all simulation runtimes, the AR 1 polymer and the AR 1:4.75 micelle exhibit the highest ε_{wall} value to which they adhere ($\varepsilon_{wall}^{critical}$). For the first mentioned polymer, that ε_{wall} value is found between 3.5 and 4, while for the second mentioned micelle, the value is found between 4.5 and 5. Another limitation present is the existence of negative, very close to 0 slopes that polymer AR 1:4.75 exhibits for ε_{wall} bigger than 5. Because of the back and forth fluctuations of the micelles after they adhere to the surface, our data appears noisy and instability arises in our results. Thus, interpolated msd values can be smaller than their predecessors, resulting in a negative slope, close to 0. In this case, the values very close to 0 can indicate that the micelles are, in fact, getting stuck. However, the slope value of -0.3 observed for the AR 1 polymer at ε_{wall} 2 (figure 9 a)) is likely an artifact, as it is not consistent with its trajectory and does not indicate that the polymer is adhering to the walls of the channel. Overall, the results of this analysis are consistent with the previous one using msd points, concluding that, in fact, polymer AR 1 and polymer AR 1:4.75 show similar behavior, traveling the longest distances before adhering to the wall. The other three also reveal similar behavior to one another, polymer 1.6:1 adhering the quickest, between ε_{wall} 2 and 3, followed by polymer 2:1 and polymer 1:3, both exhibiting a $\varepsilon_{wall}^{critical}$ value between 3 and 3.5.

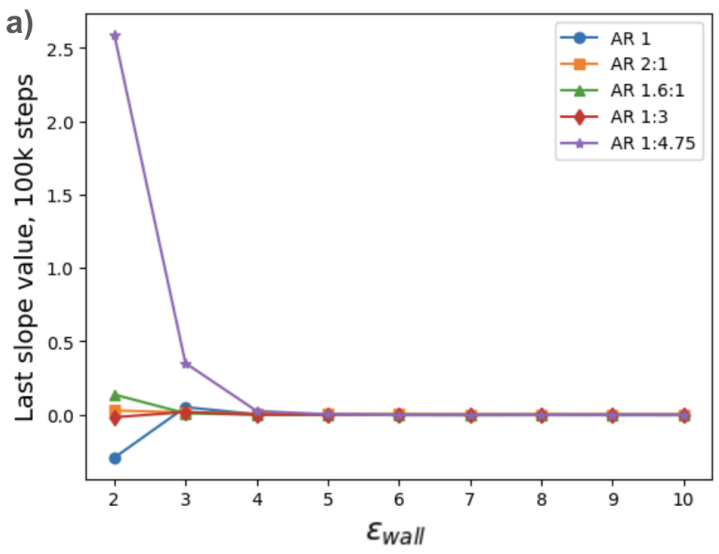
a)
Last slope value, 100k steps
AR 1
AR 2:1
AR 1.6:1
AR 1:3
AR 1:4.75
ε_{wall}

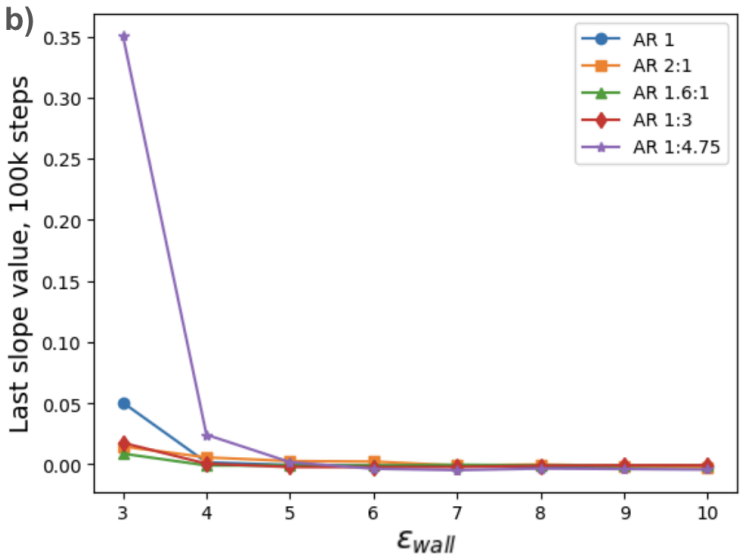
b)
Last slope value, 100k steps
AR 1
AR 2:1
AR 1.6:1
AR 1:3
AR 1:4.75
ε_{wall}

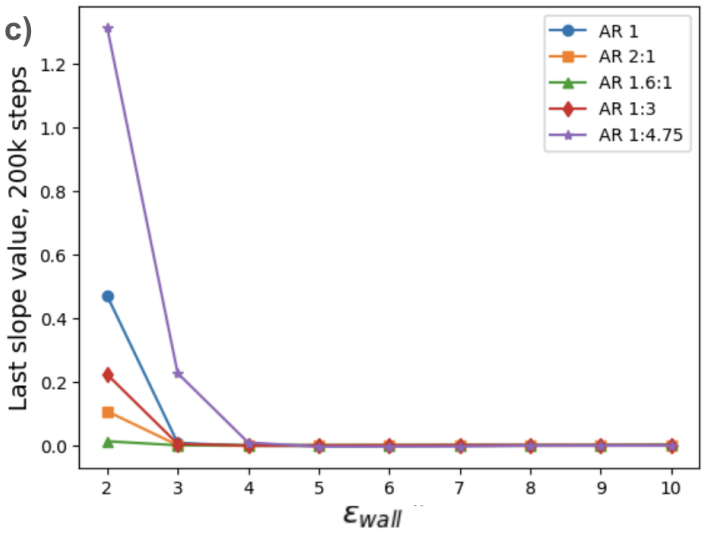
c)
Last slope value, 200k steps
AR 1
AR 2:1
AR 1.6:1
AR 1:3
AR 1:4.75
ε_{wall}

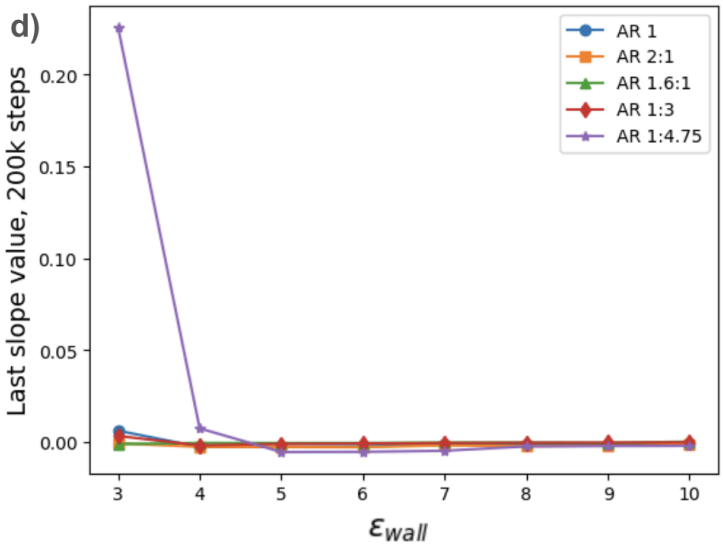
d)
Last slope value, 200k steps
AR 1
AR 2:1
AR 1.6:1
AR 1:3
AR 1:4.75
ε_{wall}

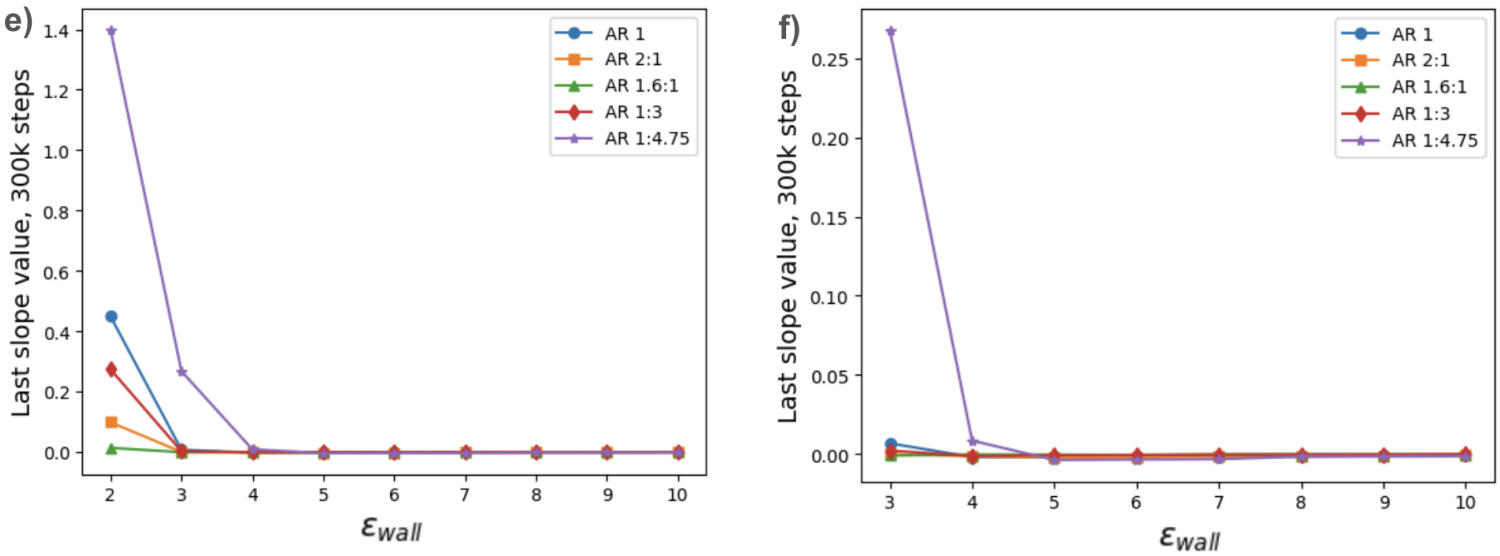

Figure 10 - Last slope values depending on ε_{wall} for all 5 polymers simulated in simulation channell 1 a) shown starting from ε_{wall} 2 obtained after 100k steps, b) shown starting from ε_{wall} 3 obtained after 100k steps, c) shown starting from ε_{wall} 2 obtained after 200k steps, d) shown starting from ε_{wall} 3 obtained after 200k steps, e) shown starting from ε_{wall} 2 obtained after 300k steps, f) shown starting from ε_{wall}n 3 obtained after 300k steps

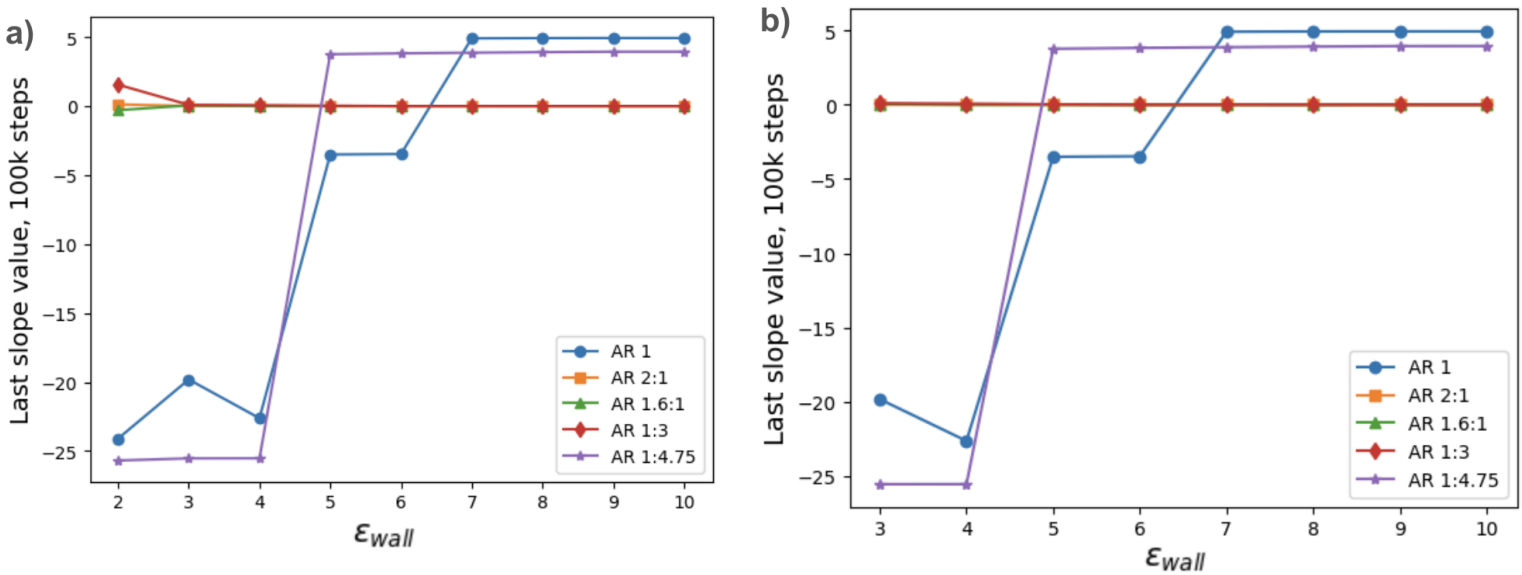

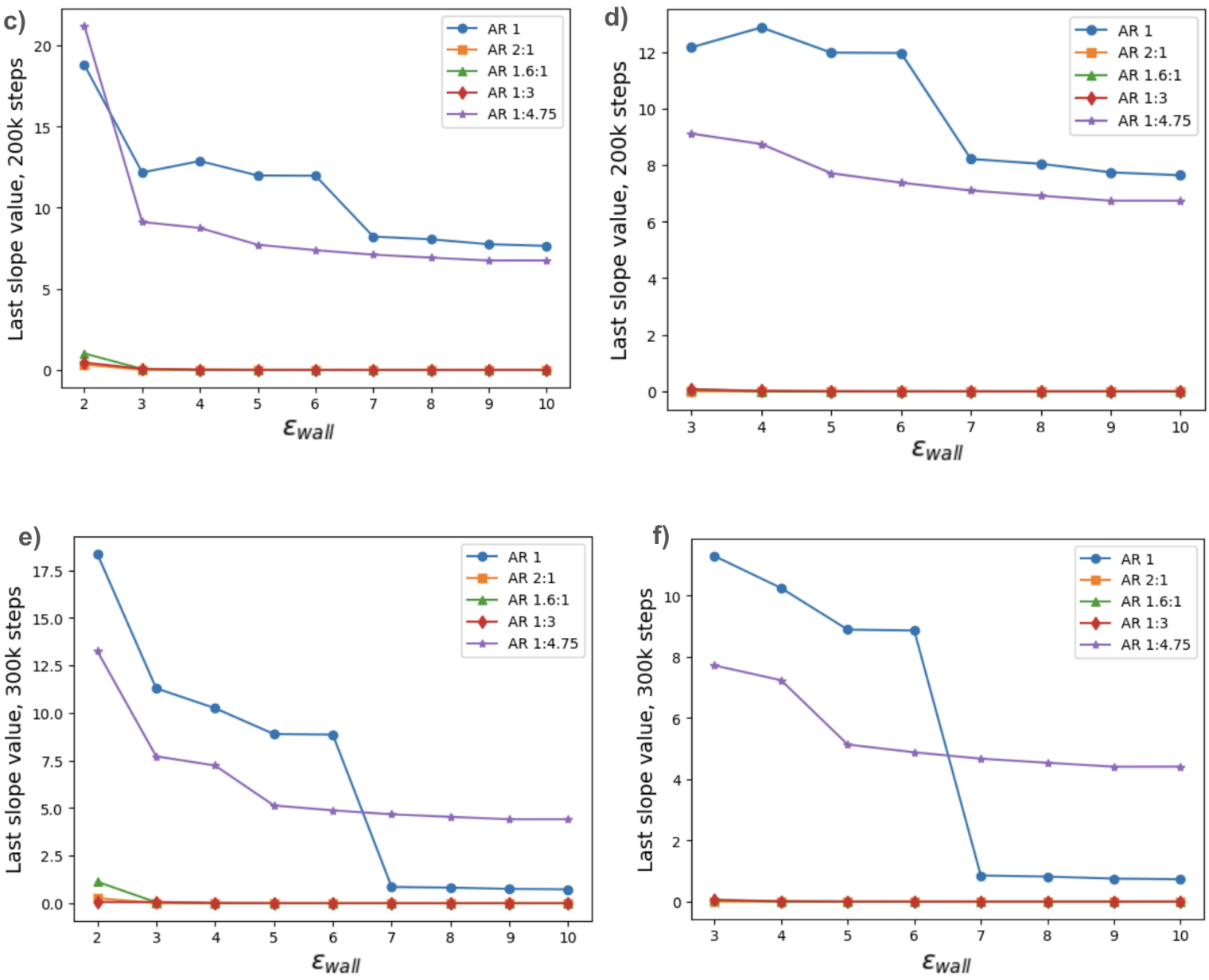

Figure 11 - Last slope values depending on ε_{wall} for all 5 polymers simulated in simulation channel 2 a) shown starting from ε_{wall} 2 obtained after 100k steps, b) shown starting from ε_{wall}n 3 obtained after 100k steps, c) shown starting from ε_{wall} 2 obtained after 200k steps, d) shown starting from ε_{wall} 3 obtained after 200k steps, e) shown starting from ε_{wall} 2 obtained after 300k steps, f) shown starting from ε_{wall} 3 obtained after 300k steps

Regarding the second channel, Figure 9 shows very high slope values for the micelles 1 and 5, but a fairly consistent behavior in time overall. Similarly to the very high slope values for $\varepsilon_{wall} = 0$

present in all graphs, the reason why polymers AR 1 and 1:4.75 illustrate high slopes for all ε_{wall} is due to the long travel time they experience before adhering to the wall . Figure A2 in the appendix illustrates the difference between time travel lengths before adhesion of polymer AR 1 and AR 1:4.75 compared to AR 2:1. Furthermore, the noise created by the back-and-forth movement of the micelles while being stuck is perceived bigger at higher orders ($> 10^3$), even if the difference in consecutive interpolated msd points while adhered is about 0.002% for all simulations. In addition to the graphs from simulations run for 100k steps, which show very low negative values that may be considered artifacts for the same two polymers, the other two time steps illustrate the micelles' adhesive behavior more consistently. Overall, micelles AR 1 and AR 4.75 seem to have the highest $\varepsilon_{wall}^{critical}$ values; however, due to the high non-zero values, these cannot be precisely determined from our calculations. Following these, polymers 1.6:1, 1, and 1:3 adhere first at ε_{wall} values between 2 and 3. As per channel 1, analyses of the msd points and interpretation of the slope values for channel 2 display similar results.

We also observe that there are still several limitations that need to be addressed. First, this is a very simplified molecular dynamics model that does not take into account the effects of chemical and thermal properties of blood on the micelles or its hydrodynamics. In addition to morphology of the micelle, its chemical compatibility with blood and its components is also an important factor to take into consideration when forming these kinds of nanoparticles. Incompatibility can result in excessive macrophage uptake and premature clearance and even early release of drug due to polymeric breakdown of the micelle. Moreover, the absorption part of the drug delivery process is only depicted here by the adherence of the polymers onto the walls of the simulation channel, which also has a rectangular shape, compared to capillaries which are cylindrical. As aforementioned, the calculation of the slopes needs to be revised and possibly redone for a more reliable generation of results. Instead of 1, a characteristic force should be computed according to the other set parameters, so altogether the simulation can reflect real life cases, not just a simplified model for better behavior assessment. For future research purposes, considerations should be addressed: running of the simulations for longer periods of time, the analysis of different channel dimensions together with micelles of other aspect ratios and incorporating multiple force flows to reflect the actual blood velocity within capillaries.

4. Conclusion

This study explores the role of micelle shape in determining its adhesive behavior in microchannels, relevant for drug delivery applications in biological systems. Our simulations demonstrated that micelles with aspect ratios 1 and 1:4.75 tend to need a higher attractive force between their atoms and the simulation channel atoms to adhere to walls more rapidly, indicating supreme retention efficiency. On the other hand, micelles with aspect ratios 1.6:1, 2:1, and 1:3 exhibit quicker adhesion, suggesting different suitability for various drug delivery scenarios. The observed high slope values and artifacts in the post processing of the simulations point to the need for more accurate modeling and longer simulation times to better capture micelle behavior. Future research should focus on refining the simulation parameters, incorporating realistic blood flow dynamics, and exploring additional micelle shapes and channel configurations. Addressing these factors will enhance our understanding of micelle behavior in drug delivery systems and improve their effectiveness in medical applications.

References

[1] *M. Ghezzi, S. Pescina, C. Padula, P. Santi, E. Del Favero, L. Cantu` and S. Nicoli, J., Polymeric micelles in drug delivery: An insight of the techniques for their characterization and assessment in biorelevant conditions. Controlled Release (2021) 332, 312–336.*

[2] *Mignani, S., Shi, X., Zablocka, M., & Majoral, J. P. (2021), Dendritic macromolecular architectures: dendrimer-based polyion complex micelles. Biomacromolecules, 22(2), 262-274.*

[3] *Zlotnikov, I. D., Streltsov, D. A., Belogurova, N. G., & Kudryashova, E. V. (2023)., Chitosan or cyclodextrin grafted with oleic acid self-assemble into stabilized polymeric micelles with potential of drug carriers. Life, 13, 446.*

[4] *Negut, I., & Bita, B. (2023), Polymeric micellar systems—a special emphasis on "smart" drug delivery. Pharmaceutics, 15, 976.*

[5] *Parra, A., Jarak, I., Santos, A., Veiga, F., & Figueiras, A. (2021), Polymeric micelles: A promising pathway for dermal drug delivery. Materials, 14, 7278.*

[6] *Chilkoti, A., Dreher, M. R., Meyer, D. E., & Raucher, D. (2002), Targeted drug delivery by thermally responsive polymers. Advanced Drug Delivery Reviews, 54, 613-630.*

[7] *Perumal, S., Atchudan, R., & Lee, W. (2022). A review of polymeric micelles and their applications. Polymers (Basel), 14(12), 2510.*

[8] *Adepu, S., & Ramakrishna, S. (2021). Controlled drug delivery systems: Current status and future directions. Molecules, 26(19), 5905.*

[9] *Zhang, Y., Huang, Y., & Li, S. (2014). Polymeric micelles: Nanocarriers for cancer-targeted drug delivery. AAPS PharmSciTech, 15(4), 862-871.*

[10] *Cabral, H., Matsumoto, Y., Mizuno, K., Chen, Q., Murakami, M., Kimura, M., Terada, Y., Kano, M. R., Miyazono, K., Uesaka, M. J., & Nishiyama, N. (2011). Nature Nanotechnology, 6(12), 815-823.*

[11] *Alexander-Bryant, A. A., Vanden Berg-Foels, W. S., & Wen, X. (2013). Bioengineering strategies for designing targeted cancer therapies. In K. D. Tew & P. B. Fisher (Eds.), Advances in Cancer Research (Vol. 118, pp. 1-59). Academic Press.*

[12] *Truong, N. P., Whittaker, M. R., Mak, C. W., & Davis, T. P. (2014). The importance of nanoparticle shape in cancer drug delivery. Expert Opinion on Drug Delivery, 12(1), 129-142.*

[13] *Chauhan, V. P., Popović, Z., Chen, O., et al. (2011). Fluorescent nanorods and nanospheres for real-time in vivo probing of nanoparticle shape-dependent tumor penetration. Angewandte Chemie, 123(48), 11619-11622.*

[14] *Zhang, S. Q., Fu, Q., Zhang, Y. J., Pan, J. X., Zhang, L., Zhang, Z. R., & Liu, Z. M. (2021). Surface loading of nanoparticles on engineered or natural erythrocytes for prolonged circulation time: Strategies and applications. Acta Pharmacologica Sinica, 42(7), 1040-1054.*

[15] *Yoo, J. W., Chambers, E., & Mitragotri, S. (2010). Factors that control the circulation time of nanoparticles in blood: Challenges, solutions and future prospects. Current Pharmaceutical Design, 16(21), 2298-2307.*

[16] *Ta, H. T., Truong, N. P., Whittaker, A. K., Davis, T. P., & Peter, K. (2018). The effects of particle size, shape, density and flow characteristics on particle margination to vascular walls in cardiovascular diseases. Expert Opinion on Drug Delivery, 15(1), 33-45.*

[17] *The Editors of Encyclopaedia Britannica. (2019, July 23). Capillary. Encyclopedia Britannica.*

[18] *Forster, J. C., Harriss-Phillips, W. M., Douglass, M. J., & Bezak, E. (2017). A review of the development of tumor vasculature and its effects on the tumor microenvironment. Hypoxia (Auckland, N.Z.), 5, 21-32*

[19] *Zhang, S. Q., Fu, Q., Zhang, Y. J., Pan, J. X., Zhang, L., Zhang, Z. R., & Liu, Z. M. (2021). Surface loading of nanoparticles on engineered or natural erythrocytes for prolonged circulation time: Strategies and applications. Acta Pharmacologica Sinica, 42(7), 1040-1054.*

[20] *Hoshyar, N., Gray, S., Han, H. B., & Bao, G. (2016). The effect of nanoparticle size on in vivo pharmacokinetics and cellular interaction. Nanomedicine, 11(6), 673-692.*

[21] *He, C. B., Hu, Y. P., Yin, L. C., Tang, C., & Yin, C. H. (2010). Effects of particle size and surface charge on cellular uptake and biodistribution of polymeric nanoparticles. Biomaterials, 31(13), 3657-3666.*

[22] *Shuvaev, V. V., Ilies, M. A., Simone, E., Zaitsev, S., Kim, Y., Cai, S. S., et al. (2011). Endothelial targeting of antibody-decorated polymeric filomicelles. ACS Nano, 5(9), 6991-6999.*

[23] *Magnani, M., Pierigè, F., & Rossi, L. (2012). Erythrocytes as a novel delivery vehicle for biologics: From enzymes to nucleic acid-based therapeutics. Therapeutic Delivery, 3(4), 405-414.*

[24] *Brahler, M., Georgieva, R., Buske, N., Muller, A., Muller, S., Pinkernelle, J., et al. (2006). Magnetite-loaded carrier erythrocytes as contrast agents for magnetic resonance imaging. Nano Letters, 6(11), 2505-2510.*

[25] *Muzykantov, V. R. (2010). Drug delivery by red blood cells: Vascular carriers designed by mother nature. Expert Opinion on Drug Delivery, 7(4), 403-427.*

[26] *Discher, D. E. (2008). Shape effects of filaments versus spherical particles in flow and drug delivery. In Proceedings of the ASME 2008 Summer Bioengineering Conference, Parts A and B (pp. 739). Marco Island, Florida, USA.*

[27] *Hadji, H., & Bouchemal, K. (2022). Effect of micro- and nanoparticle shape on biological processes. Journal of Controlled Release, 342, 93-110.*

[28] *Ezike, T. C., Okpala, U. S., Onoja, U. L., Nwike, C. P., Ezeako, E. C., Okpara, O. J., Okoroafor, C. C., Eze, S. C., Kalu, O. L., Odoh, E. C., Nwadike, U. G., Ogbodo, J. O., Umeh, B. U., & Ossai, E. C. (2023). Advances in drug delivery systems, challenges and future directions. Heliyon, 9(6), e17488.*

[29] *Sakamoto, Y., Fujii, S., Takano, S., Fukushima, J., Ando, M., Kodera, N., & Nishimura, T. (2024). Manipulation of macrophage uptake by controlling the aspect ratio of graft copolymer micelles. Nano Letters, 24.*

[30] *Goraya, S. A., Ding, S., Miller, R. C., Arif, M. K., Kong, H., & Masud, A. (2024). Modeling of spatiotemporal dynamics of ligand-coated particle flow in targeted drug delivery processes. Proceedings of the National Academy of Sciences, 121(22), e2314533121*

[31] *Tuckerman, M. E., & Martyna, G. J. (2000). Understanding modern molecular dynamics: Techniques and applications. The Journal of Physical Chemistry B, 104(2), 159-178.*

[32] *Durrant, J. D., & McCammon, J. A. (2011). Molecular dynamics simulations and drug discovery. BMC Biology, 9(71).*

[33] *Alexander Stukowski 2010 Modelling Simul. Mater. Sci. Eng. 18 015012*

[34] *LAMMPS - a flexible simulation tool for particle-based materials modeling at the atomic, meso, and continuum scales, A. P. Thompson, H. M. Aktulga, R. Berger, D. S. Bolintineanu, W. M. Brown, P. S. Crozier, P. J. in 't Veld, A. Kohlmeyer, S. G. Moore, T. D. Nguyen, R. Shan, M. J. Stevens, J. Tranchida, C. Trott, S. J. Plimpton, Comp Phys Comm, 271 (2022) 10817.*

[35] *Pollock, F., & Blum, J. J. (1966). On the distribution of a permeable solute during Poiseuille flow in capillary tubes. Biophysical Journal, 6(1), 19-28.*

[36] *Adorf, C. S., Dodd, P. M., Ramasubramani, V., & Glotzer, S. C. (2018). Simple data and workflow management with the signac framework. Computational Materials Science, 146, 220–229.*

Appendix

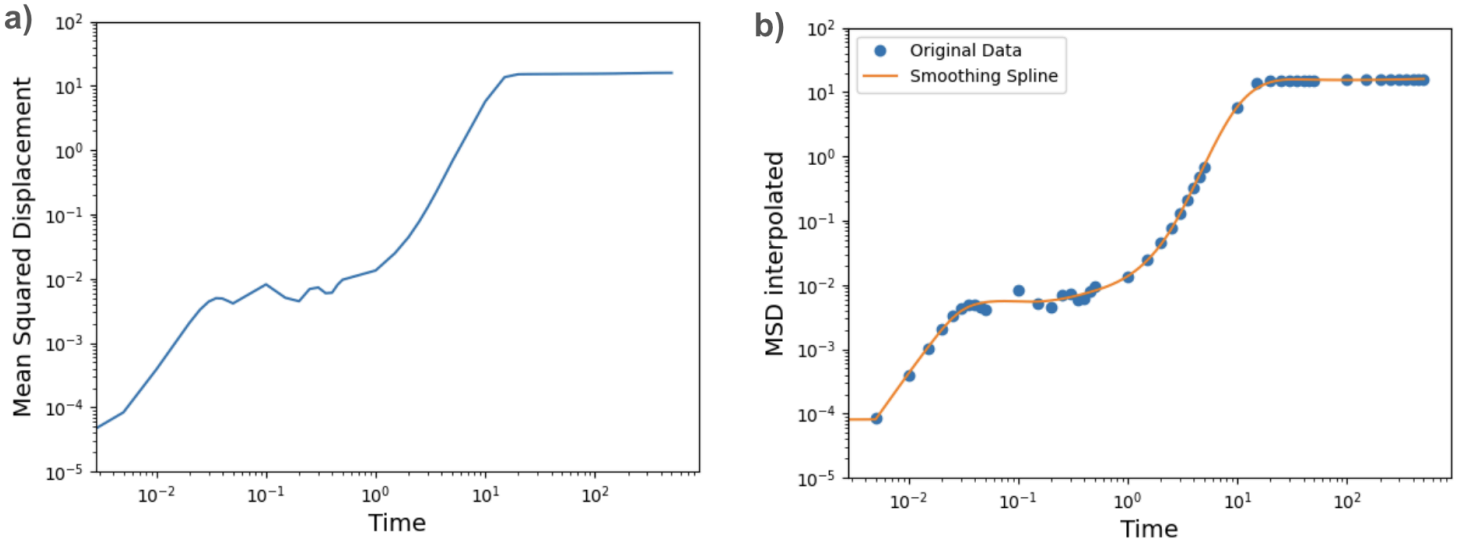

Figure A1- difference between plotted MSD points seen in a) and plotted interpolated MSD points of micelle AR1, ε_{wall} = 4 which result in a smooth spline seen in b); simulation performed in channel 1 at 100k steps

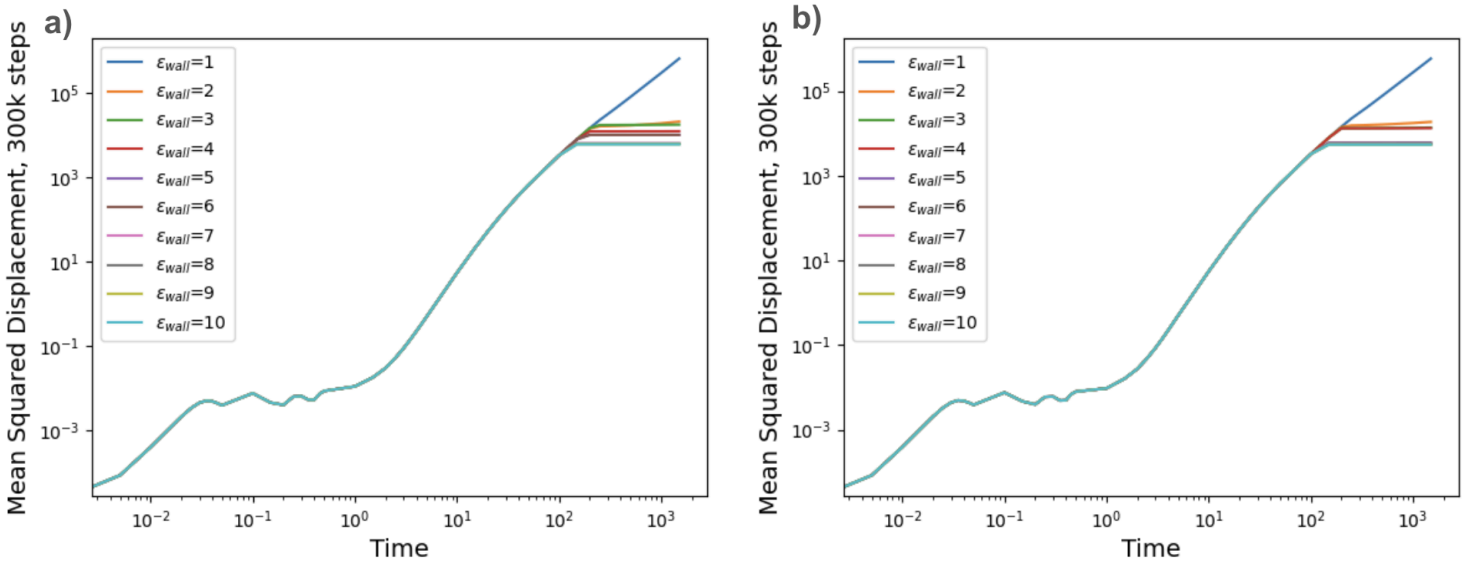

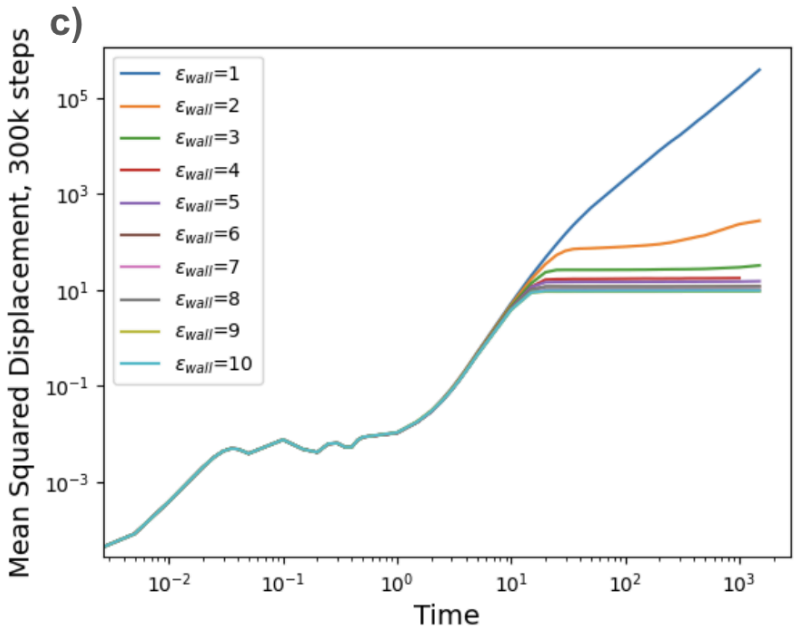

Figure A2 - difference between MSD values after adhesion between micelles AR 1, 1:4.75 compared to micelle AR 2:1; simulation performed in channel 2, 300k steps